ELSEVIER

Journal of Applied Geophysics 50 (2002) 217–229

JOURNAL OF APPLIED GEOPHYSICS

www.elsevier.com/locate/jappgeo

One-dimensional modelling for proton magnetic resonance sounding measurements over an electrically conductive medium

Pierre Valla [a,*], Anatoly Legchenko [b]

[a] *IRIS-Instruments, BP 6007, 45060 Orléans Cedex, France*
[b] *BRGM, Direction de la recherche, BP 6009, 45060 Orléans Cedex, France*

Abstract

The theory of the proton magnetic resonance sounding (a.k.a. surface nuclear magnetic resonance) was first developed in free space. In this case, the alternative excitation field has no phase variation. Hence there is no major difficulty in determining the effect of its active component, that is the one perpendicular to the static field. But over a conductive medium, the excitation field induces eddy currents, resulting in a secondary field that also has to be considered. The computation made up to now in this case did not consider the detailed physical behaviour of an excitation field which is elliptically polarised: only an extrapolation of the linearly polarised case was made which turns out to be only an approximation. This paper presents the proper formalism that permits to take rigorously into account the effect of the elliptically polarised field on the rotation of the magnetic moment of the protons, so as to obtain the correct derivation of the magnetic resonance signal produced. When compared with the approximate algorithm previously used for 1D modelling, computation results show that no significant differences arise for resistivities as low as 1 Ω m. It is only for a 2D water distribution in a medium with a 1D geoelectrical structure that differences can be observed.

Keywords: One-dimensional modelling; Proton magnetic resonance sounding measurements; Electrically conductive medium

1. Introduction

The theory of nuclear magnetic resonance (NMR) states that only the component of the energising alternative field that is perpendicular to the static field actually excites the protons and makes their magnetic moment tilt away from the static magnetic field orientation. In free space where the electrical conductivity is zero everywhere, the energising alternative field has a well-defined orientation at each point as it is linearly polarised. In such a case, there is no difficulty in defining and computing its component in the plane perpendicular to the static field for further evaluation of the NMR effect (Legchenko and Valla, this issue). In the presence of a conductive medium, the protons are energised by the total field that is the sum of the primary field and of the secondary field due to induced currents in the conductive medium. It is known that such a total field follows an ellipse due to the phase differences between its various components: it is elliptically polarised. The projection of such an ellipse onto the plane perpendicular to the static field is also an ellipse. In such a case, it is not obvious which component of the magnetic field has to be taken for the NMR behaviour.

* Corresponding author. 57 blvd. Alexandre Martin, 45000 Orléans, France.
E-mail address: pierre.valla@mines.org (P. Valla).

0926-9851/02/$ - see front matter
PII: S0926-9851(02)00141-6

The aim of this paper is to present the proper formalism for determining the effect of the elliptically polarised field on the tilting of the magnetic moment of the protons so as to obtain the correct expression of the NMR signal produced from underground water. Also the effect of the conductive medium on the NMR relaxation signal on its way back to the surface receiver has to be taken into account. This problem has already been investigated by Trushkin et al. (1995); however their results have been obtained through an approximate expression as will be shown hereafter. The first published, detailed analysis is that of Weichman et al. (1999): our approach is similar, while trying to keep as close as possible to standard notations used in geoelectromagnetic methods of applied geophysics.

We will use the same notations as in the previous paper by Legchenko and Valla (this issue):

ω_0	is the angular Larmor frequency
γ	is the gyromagnetic ratio of protons
M_0	is the nuclear magnetisation of protons
$w(p)$	is the water content distribution
$T_2^*(p)$	is the decay time constant distribution
$b_\perp^{\mathrm{Rx}}(p)$	is the transverse part of the reciprocal magnetic induction field created at point p by a unit current in the receiver loop
$b_\perp^{\mathrm{Tx}}(p)$	is the transverse part of the magnetic induction field created at point p by the transmitter loop, normalised to a unit current
q	is the moment of the energising pulse

Considering the case of a half-space made of horizontal electrically conductive layers, the question is to find out which modifications are to be made in the basic equation of the surface nuclear magnetic resonance (SNMR) geophysical technique, giving the transient decay voltage response in the receiver loop

$$E(t) = -\int_V \omega_0 M_0 \times w(p) b_\perp^{\mathrm{Rx}}(p) \sin\left(\frac{1}{2}\gamma b_\perp^{\mathrm{Tx}}(p) q\right) \times \mathrm{e}^{-t/T_2^*(p)} \mathrm{d}V(p) \quad \text{(E)}$$

as derived in the case of free space (resistive host rock).

2. The electromagnetic field of a loop above electrically conductive layers

If the transmitter–receiver loop was approximated by a vertical magnetic dipole of moment $M = I\pi a^2$, its magnetic induction field would be expressed as (Kaufman and Keller, 1983; Wait, 1982)

$$\boldsymbol{B}(p) = \mu[i\omega\mu\sigma(p)\boldsymbol{F}(p) - \mathrm{grad}(\mathrm{div}(\boldsymbol{F}(p)))] \quad (1)$$

where $\boldsymbol{F}$ is a Hertz potential which has only a vertical non-zero component, expressed as a Hankel transform

$$F_z(r,z) = \frac{M}{4\pi}\int_0^\infty K_\mathrm{d}(\lambda,z)\lambda J_0(\lambda r)\mathrm{d}\lambda \quad (2)$$

of some kernel function which, in the jth layer with the conductivity σ_j, can be written as

$$K_\mathrm{d}(\lambda,z) = a_j(\lambda)\mathrm{e}^{+m_j z} + b_j(\lambda)\mathrm{e}^{-m_j z} \quad (3)$$

where $m_j = \sqrt{\lambda^2 + i\omega\mu\sigma_j}$, and the coefficients $a_j(\lambda)$ and $b_j(\lambda)$ are recursively determined.Then the non-zero components of the magnetic induction field would be

$$B_r = \frac{\mu M}{4\pi}\int_0^\infty \frac{\partial K_\mathrm{d}(\lambda,z)}{\partial z}\lambda^2 J_1(\lambda r)\mathrm{d}\lambda \quad (4.1)$$

$$B_z = -\frac{\mu M}{4\pi}\int_0^\infty K_\mathrm{d}(\lambda,z)\lambda^3 J_0(\lambda r)\mathrm{d}\lambda. \quad (4.2)$$

If the loop is now considered with its true finite radius a, the kernel must be changed to the following (Ryu et al., 1970; Wait, 1982)

$$K_{\mathrm{loop}}(\lambda,z) = \frac{J_1(\lambda a)}{\lambda a/2}K_\mathrm{d}(\lambda,z) \quad (5)$$

so that the components of the magnetic induction field are

$$B_r = \frac{\mu I a}{2}\int_0^\infty \frac{\partial K_\mathrm{d}(\lambda,z)}{\partial z}\lambda J_1(\lambda a)J_1(\lambda r)\mathrm{d}\lambda \quad (6.1)$$

$$B_z = -\frac{\mu I a}{2}\int_0^\infty K_\mathrm{d}(\lambda,z)\lambda^2 J_1(\lambda a)J_0(\lambda r)\mathrm{d}\lambda. \quad (6.2)$$

One might think that the computation of the proton magnetic response is then straightforward, by using the above formulas to determine the $b_{\perp}^{\mathrm{Tx}}$ and $b_{\perp}^{\mathrm{Rx}}$ fields of formula (E) as for the resistive case. This is not completely so because those fields are elliptically polarised, due to the secondary field of the conductive layers. Hence in most cases the $\boldsymbol{B}^{\mathrm{Tx}}$ field, once projected upon the plane perpendicular to $\boldsymbol{B}_0$ will still be elliptically polarised and the question is to investigate the ellipticity effects on the solution of the Bloch equations.

3. Magnetic resonance with elliptically polarised energising fields

The transverse part of an elliptically polarised field $\boldsymbol{B}_{\perp}^{\mathrm{Tx}}$, can be written as the sum of left (clockwise in the x–y plane) and the right (counter-clockwise) circularly polarised rotating fields, namely

$$\begin{aligned}\boldsymbol{B}_{\perp}^{\mathrm{Tx}} &= \boldsymbol{u}_z \times (\boldsymbol{B}^{\mathrm{Tx}} \times \boldsymbol{u}_z) \\ &= B_{x'}^{\mathrm{Tx}} \frac{1}{2}(\boldsymbol{u}_{x'}^{+} + \boldsymbol{u}_{x'}^{-}) + B_{y'}^{\mathrm{Tx}} \frac{1}{2}(\boldsymbol{u}_{y'}^{+} + \boldsymbol{u}_{y'}^{-}) \end{aligned} \tag{7}$$

where $\boldsymbol{u}_{x'}^{+}$ and $\boldsymbol{u}_{y'}^{+}$ are the unit vectors of the co-rotating frame of reference (rotating clockwise at angular frequency ω_0 around $\boldsymbol{u}_z$), and $\boldsymbol{u}_{x'}^{-}$ and $\boldsymbol{u}_{y'}^{-}$ are the counter-rotating unit vectors

$$\boldsymbol{u}_{x'}^{+} = \cos(\omega_0 t)\boldsymbol{u}_x - \sin(\omega_0 t)\boldsymbol{u}_y \tag{8.1}$$

$$\boldsymbol{u}_{x'}^{-} = \cos(\omega_0 t)\boldsymbol{u}_x + \sin(\omega_0 t)\boldsymbol{u}_y \tag{8.2}$$

$$\boldsymbol{u}_{x'}^{-} = \cos(\omega_0 t)\boldsymbol{u}_y + \sin(\omega_0 t)\boldsymbol{u}_x \tag{8.3}$$

$$\boldsymbol{u}_{y'}^{-} = \cos(\omega_0 t)\boldsymbol{u}_y - \sin(\omega_0 t)\boldsymbol{u}_x. \tag{8.4}$$

The coefficients $B_{x'}^{\mathrm{Tx}}$ and $B_{y'}^{\mathrm{Tx}}$ are complex numbers including a phase information. Only the co-rotating components produce a non-zero time-averaged torque on the magnetisation of the protons. It is this component that enters the Bloch equation (Eq. (E)), as the "active" component; the counter-rotating component averages to zero and is "inactive".

We will first investigate the case of a linearly polarised dephased field in the rotating x' –y' frame by assuming

$$\begin{aligned}\boldsymbol{B}_{\perp}^{\mathrm{Tx}} &= Re(B_{\perp}^{\mathrm{Tx}} \mathrm{e}^{i(\omega_0 t+\phi)})\boldsymbol{u}_x \\ &= B_{\perp}^{\mathrm{Tx}}(\cos(\omega_0 t)\cos(\phi) \\ &\quad - \sin(\omega_0 t)\sin(\phi))\boldsymbol{u}_x. \end{aligned} \tag{9}$$

Then

$$\begin{aligned}\boldsymbol{B}_{\perp}^{\mathrm{Tx}} &= B_{\perp}^{\mathrm{Tx}}\cos(\phi)\frac{1}{2}(\boldsymbol{u}_{x'}^{+} + \boldsymbol{u}_{x'}^{-}) \\ &\quad - B_{\perp}^{\mathrm{Tx}}\sin(\phi)\frac{1}{2}(\boldsymbol{u}_{y'}^{+} - \boldsymbol{u}_{y'}^{-}) \end{aligned} \tag{10}$$

so that this case is similar to the resistive host one studied by Legchenko and Valla (this issue) if we set

$$\boldsymbol{u}_{\perp} = \cos(\phi)\boldsymbol{u}_{x'}^{+} - \sin(\phi)\boldsymbol{u}_{y'}^{+}. \tag{11}$$

The phase ϕ results in a rotation of the perpendicular "active" induction field by an angle $-\phi$. The resulting transverse component of the magnetisation vector is

$$\begin{aligned} &M_{x'}\boldsymbol{u}_{x'}^{+} + M_{y'}\boldsymbol{u}_{y'}^{+} \\ &\quad = M_{\perp}Re\Big[\Big((\cos(\phi)\boldsymbol{u}_y + \sin(\phi)u_x) \\ &\qquad - i(\cos(\phi)\boldsymbol{u}_x - \sin(\phi)\boldsymbol{u}_x)\Big)\mathrm{e}^{i\omega_0 t}\Big] \\ &\quad = M_{\perp}Re\Big(\mathrm{e}^{i\phi}(\boldsymbol{u}_y - i\boldsymbol{u}_x)\mathrm{e}^{i\omega_0 t}\Big) \\ &\quad = M_{\perp}Re\Big(\mathrm{e}^{i\phi}(\boldsymbol{u}_{y'}^{+} - i\boldsymbol{u}_{x'}^{+})\Big). \end{aligned} \tag{12}$$

If the receiver antenna is the same as the transmitter antenna, then

$$\begin{aligned} B_{\perp}^{\mathrm{Rx}} &= \langle i\boldsymbol{B}^{\mathrm{Tx}}, \mathrm{e}^{i\phi}(\boldsymbol{u}_y - i\boldsymbol{u}_x)\rangle \\ &= \langle B_{\perp}^{\mathrm{Tx}}\mathrm{e}^{i\phi}\boldsymbol{u}_x, \mathrm{e}^{i\phi}(\boldsymbol{u}_x + i\boldsymbol{u}_y)\rangle = B_{\perp}^{\mathrm{Tx}}\mathrm{e}^{2i\phi} \end{aligned} \tag{13}$$

where $\langle\ ,\ \rangle$ is the complex scalar product. This result is the same as Eq. (1) of Trushkin et al. (1995) and Eq. (11) of Shushakov (1996).

We will now come back to the general case of an elliptically polarised field. When using both the ($\boldsymbol{u}_{x'}^{+}$, $\boldsymbol{u}_{y'}^{+}$) co-rotating frame of reference in the x–y plane and

complex numbers to deal with harmonic time-varying functions, we have the following identities

$$\cos(\omega_0 t)\boldsymbol{u}^+_{x'} + \sin(\omega_0 t)\boldsymbol{u}^+_{y'} = \boldsymbol{u}_x = \mathrm{e}^{-i\omega_0 t}\boldsymbol{u}^+_{x'} = \cos(\omega_0 t)\boldsymbol{u}^+_{x'} - i\sin(\omega_0 t)\boldsymbol{u}^+_{x'} \quad (14.1)$$

$$\cos(\omega_0 t)\boldsymbol{u}^-_{x'} - \sin(\omega_0 t)\boldsymbol{u}^-_{y'} = \boldsymbol{u}_x = \mathrm{e}^{+i\omega_0 t}\boldsymbol{u}^-_{x'} = \cos(\omega_0 t)\boldsymbol{u}^-_{x'} + i\sin(\omega_0 t)\boldsymbol{u}^-_{x'} \quad (14.2)$$

and as a special case,

$$\boldsymbol{u}^+_{y'} = -i\boldsymbol{u}^+_{x'} \quad (15.1)$$

$$\boldsymbol{u}^-_{y'} = +i\boldsymbol{u}^-_{x'} \quad (15.2)$$

meaning that the complex numbers can also be considered as operating in the space domain of the complex $z=x+iy$ plane. Hence the transverse part of the magnetic induction generated by the transmitter can be expressed as

$$\boldsymbol{B}^{\mathrm{Tx}}_{\perp} = \frac{1}{2}(B^{\mathrm{Tx}}_{x'} - iB^{\mathrm{Tx}}_{y'})\boldsymbol{u}^+_{x'} + \frac{1}{2}(B^{\mathrm{Tx}}_{x'} + iB^{\mathrm{Tx}}_{y'})\boldsymbol{u}^-_{x'} \quad (16)$$

which is the sum of the co-rotating and counter-rotating parts. Since the "active" component is the $\boldsymbol{u}^+_{x'}$ one, writing

$$B^{\mathrm{Tx}}_{x'} - iB^{\mathrm{Tx}}_{y'} = \left|B^{\mathrm{Tx}}_{x'} - iB^{\mathrm{Tx}}_{y'}\right|\exp(i\phi_{\mathrm{Tx}}) \quad (17)$$

we get

$$B^{\mathrm{Tx}}_{\perp} = \left|B^{\mathrm{Tx}}_{x'} - iB^{\mathrm{Tx}}_{y'}\right| \quad (18)$$

and

$$B^{\mathrm{Rx}}_{\perp} = \langle i\boldsymbol{B}^{\mathrm{Rx}}, \exp(i\phi_{\mathrm{Tx}})(\boldsymbol{u}_y - i\boldsymbol{u}_x)\rangle = (B^{\mathrm{Rx}}_{x'} + iB^{\mathrm{Rx}}_{y'})\exp(i\phi_{\mathrm{Tx}}). \quad (19)$$

Those are the relationships to be used within Eq. (E) for the general case of a conductive Earth, with separate transmitter and receiver antennas. We observe that while the module of the co-rotating Tx field is to be taken into account in the sine function for getting the amplitude of the relaxation dipolar moment, it is the counter-rotating (reciprocal) Rx field which has to be used for computing the induced field of this moment.

4. Discussion of the local physical behaviour

From the above it follows that the general magnetic resonance upon an electrically conductive layered half-space is

$$E(t) = -\int_V \omega_0 M_0 \times w(p) b^{\mathrm{Rx}}_{\perp}(p)\mathrm{e}^{i\phi_{\mathrm{Tx}}(p)} \times \sin\left(\frac{1}{2}\gamma b^{\mathrm{Tx}}_{\perp}(p)q\right)\mathrm{e}^{-t/T_2^*(p)}\mathrm{d}V(p) \quad (E')$$

where

$$b^{\mathrm{Tx}}_{\perp} = \left|b^{\mathrm{Tx}}_x - ib^{\mathrm{Tx}}_y\right| \quad (20.1)$$

$$\phi_{\mathrm{Tx}} = \arg(b^{\mathrm{Tx}}_x - ib^{\mathrm{Tx}}_y) \quad (20.2)$$

$$b^{\mathrm{Rx}}_{\perp} = \langle \boldsymbol{b}^{\mathrm{Rx}}, \boldsymbol{u}_x + i\boldsymbol{u}_y\rangle \quad (20.3)$$

for an arbitrary x–y right-handed coordinate system in the plane orthogonal to the static magnetic induction field $\boldsymbol{B}_0$.

If we select the x–y coordinates such that $\boldsymbol{u}_x$ is along the major axis of the polarisation ellipse and $\boldsymbol{u}_y$ is along a minor axis, then we can try and get a physical understanding of formula (20.1) here above. There are basically two cases, which are depicted in Fig. 1: in the orthogonal plane, either the energising induction field runs clockwise along the polarisation ellipse or it runs counter-clockwise. In the first instance, the minor axis component strengthens the action of the major axis component by creating a stronger co-rotating field which is the "active" part in the Bloch equations; in the second instance, the minor axis component weakens the action of the major axis component by taking away a part of it for strengthening the counter-clockwise rotating field which is an "inactive" part in the Bloch equations. Since

$$a_x\cos(\omega_0 t)\boldsymbol{u}_x + a_y\sin(\omega_0 t)\boldsymbol{u}_y = Re\left((a_x u_x - ia_y\boldsymbol{u}_y)\mathrm{e}^{i\omega_0 t}\right) \quad (21)$$

it can be checked that in the first instance b^{Tx}_y will be a positive imaginary number assuming b^{Tx}_x is a positive real one, hence

$$b^{\mathrm{Tx}}_{\perp} = \left|b^{\mathrm{Tx}}_x - ib^{\mathrm{Tx}}_y\right| = \left|b^{\mathrm{Tx}}_x\right| + \left|b^{\mathrm{Tx}}_y\right| \quad (22.1)$$

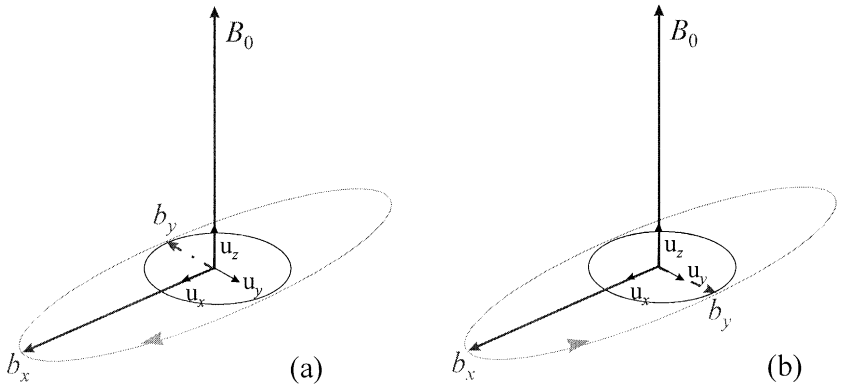

Fig. 1. An elliptically polarised induction field $\boldsymbol{b}$ rotating clockwise (a) or counter-clockwise (b) around the static geomagnetic field $\boldsymbol{B}_0$.

while in the second instance b_y^{Tx} will be a negative imaginary number, hence

$$b_{\perp}^{\mathrm{Tx}} = \left|b_x^{\mathrm{Tx}} - ib_y^{\mathrm{Tx}}\right| = \left|b_x^{\mathrm{Tx}}\right| - \left|b_y^{\mathrm{Tx}}\right|. \qquad (22.2)$$

5. Numerical implementation and accuracy evaluation

While the computation in the resistive case can be performed with a standard polynomial approximation of the elliptical functions and numerical quadrature, the Hankel transform giving the magnetic induction field of a loop require specific numerical algorithms. The most widely used one is the lagged convolution filtering technique devised by Anderson (1979). However its accuracy for computing fields inside the conductive half-space has been questioned by Chave (1983). Hence a comparison has been made with a computation using a refined filter and even direct adaptive numerical quadrature as soon as the oscillatory behaviour of the kernel is too high, as proposed by Anderson (1989). The comparison is made on Figs.

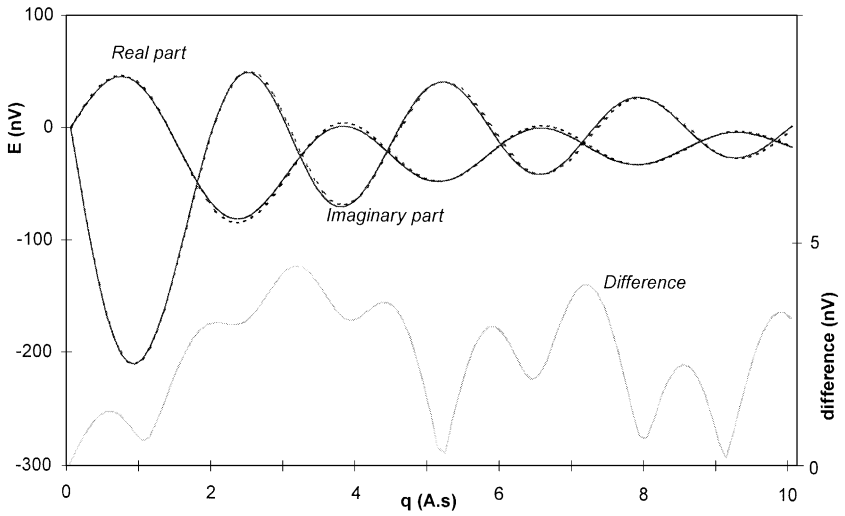

Fig. 2. Response of a thin (1 m) water layer at 10 m depth in a 1 Ω m host medium computed through a refined algorithm (solid lines) and standard filter (dashed line); the antenna is a circular loop with 100 m diameter.

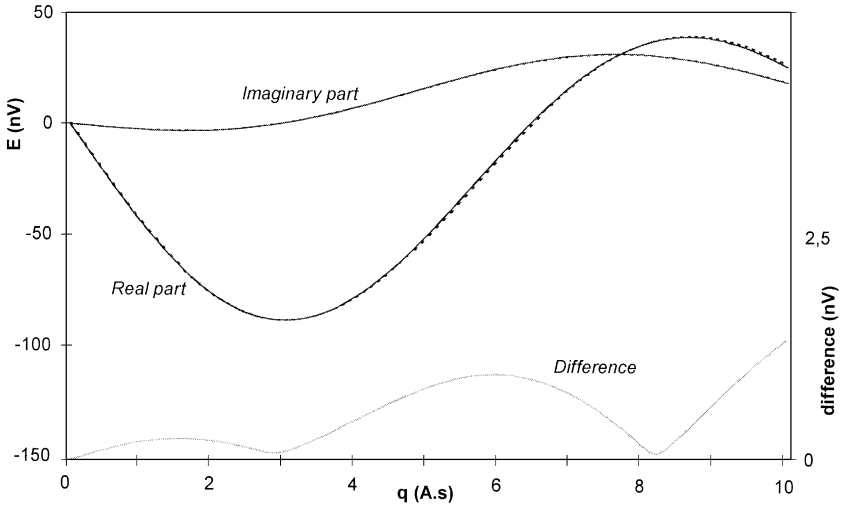

Fig. 3. Response of a thin (1 m) water layer at 20 m depth in a 1 Ω m host medium computed through a refined algorithm (solid lines) and standard filter (dashed line); the antenna is a circular loop with 100 m diameter.

2 and 3 for the magnetic resonance response of a thin layer sited at a depth of either 10 or 20 m, within a 1-Ω m half-space at 60° geomagnetic field inclination with a 50,000 nT magnitude; the transmitter and receiver antennas are coincident, being a circular loop with a diameter of 100 m. The differences between the two calculations can barely be seen on the simultaneous graphical plot: the difference is only a few percent of the maximum amplitude. The relative difference becomes significant only for the lower amplitude parts of the response. This is of no consequence in the inversion process as it is limited by a measurement noise that is of rather stable absolute value. Thus for all practical needs the standard Anderson's filter will be quite adequate.

6. Thin layer responses for various host medium resistivity

Using the above described numerical algorithm, the amplitude response of a thin water layer—"thin" meaning that the thickness is small compared to the depth—has been computed for various host medium resistivity (1, 3, 10 and 100 Ω m), various depth of the water layer (20, 35 and 50 m) and various geomagnetic field inclination (0°, 30°, 60° and 90°). The loop diameter is 100 m. The geomagnetic field strength has been varied as a function of the inclination according to the dipole formula. The results are plotted on Figs. 4 and 5.

It is observed that for a host medium resistivity higher than 100 Ω m, little change occurs compared to the infinitely resistive case. In the 10 Ω m range the amplitude of the response gets lower when the water layer is below 30 m depth, but the shape of the first lobe is still similar. But for still lower resistivities, the effect becomes stronger. For a resistivity of 3 Ω m, the response of a 50-m deep water layer is similar to the response of a 100-m deep water layer sited in a infinitely resistive host; this means that the depth of investigation is divided by two. For a resistivity of 1 Ω m, it is divided by three.

7. Differences between the results from the approximate and exact formulas

Various computations have been performed to assess the error introduced by the approximate formula of Trushkin et al. (1995) and Shushakov (1996). It has been found that significant differences with the exact formula occur only for combined low values of the geomagnetic field inclination, quite low resistivity

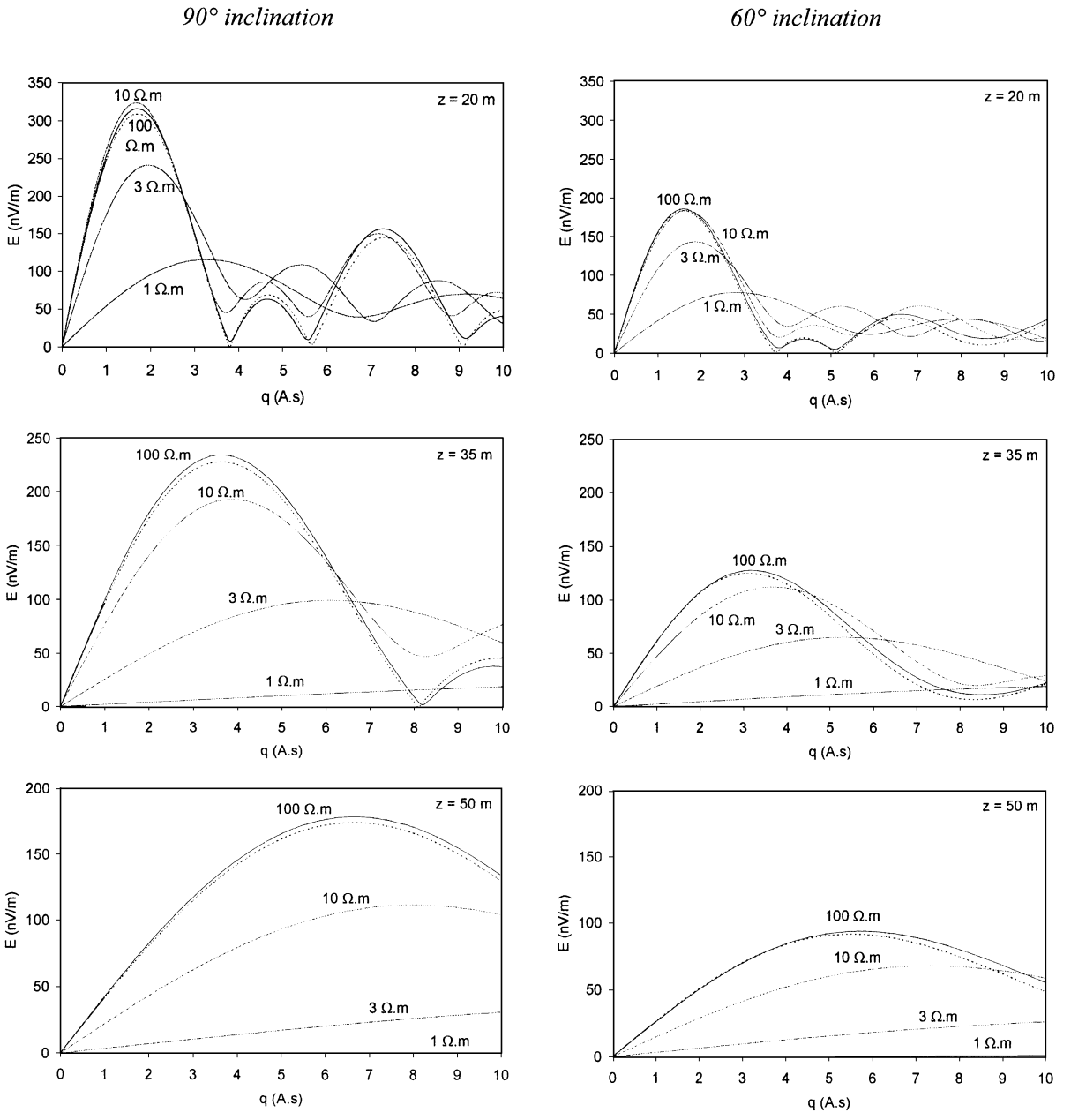

Fig. 4. Amplitude response of a thin water layer for various electrical resistivity of the host medium; dashed curve is for free space (infinitely resistive), solid curves are for 100, 10, 3 and 1 Ω m resistivity; the left hand side plots are for a 90° inclination with a 60,000 nT geomagnetic field; the right hand side plots are for a 60° inclination with a 45,360 nT geomagnetic field; water layer depths are 20 (top), 35 (middle) and 50 m (bottom).

(1 Ω m or lower) and shallow water layers This is illustrated by Fig. 6 where the results from the two formulas are compared for a thin water layer sited at 10 and 20 m depth within a 1 Ω m half-space at 0° inclination with a 50,000 nT magnitude. The error does not exceed 8% of the maximum value of the

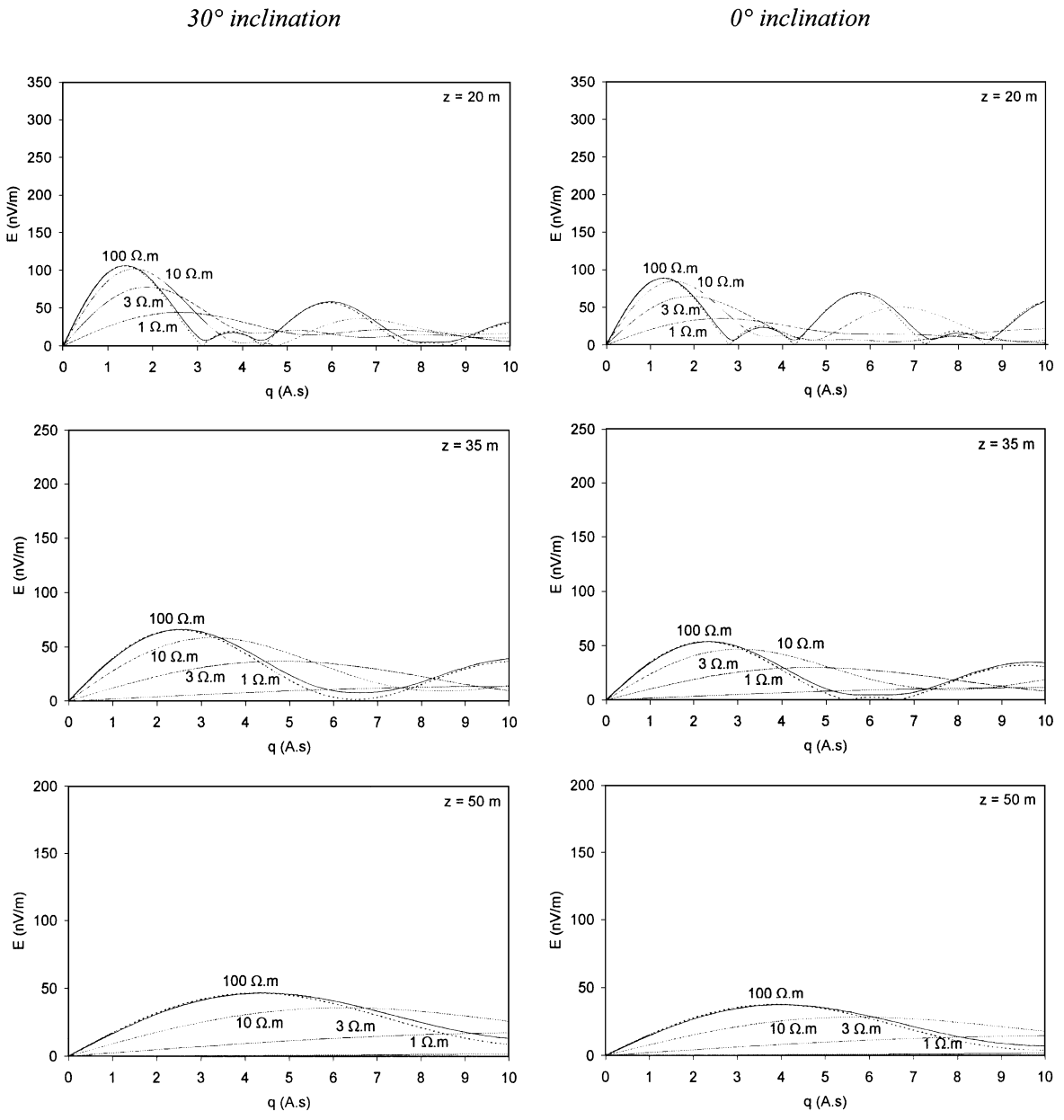

Fig. 5. Amplitude response of a thin water layer for various electrical resistivity of the host medium; dashed curve is for free space (infinitely resistive), solid curves are for 100, 10, 3 and 1 Ω m resistivity, the left hand side plots are for a 30° inclination with a 33, 280 mT geomagnetic field; the right hand side plots are for a 0° inclination with a 30,000 mT geomagnetic field; water layers depths are 20 (top), 35 (middle) and 50 m (bottom).

response and does not affect the starting part of the curve. Hence no major bias in the inversion is to be expected when the approximate formula is being used instead of the exact one. The differences are even smaller at higher latitudes since the energising field is close to being linearly polarised: indeed at the poles where the geomagnetic field is vertical, only the radial component of the magnetic induction field created by

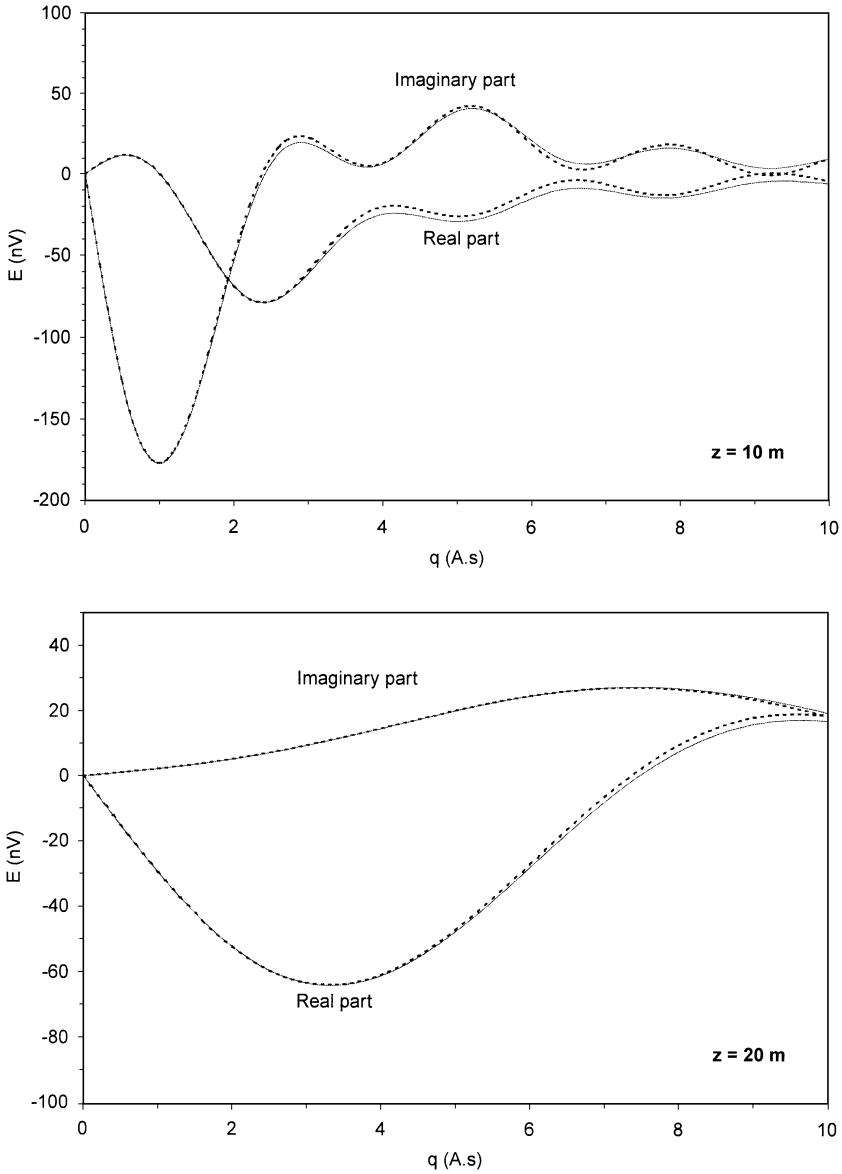

Fig. 6. Comparison of computation made using the approximate (dashed line) and exact (solid line) algorithms for a thin (1 m) water layer at 10 (top) and 20 m (bottom) depth within a 1 Ω m half-space at 0° inclination.

the circular transmitter loop is energising the water protons, so that we are in the linear polarisation case with no differences between the approximate and exact formulas. This is why the inaccuracy could not be identified by Trushkin et al. (1995) who compared theoretical results and field tests made primarily at high northern latitudes.

8. Analysis of a simple 2D case

The fact that the differences between the results from the approximate and exact formulas are small for 1D configurations does not mean that the same conclusion is true for 2D configurations. For the 1D case, the differences are, in fact, averaged out because at

locations that are symmetrical with respect to the vertical meridian plane, the ellipse will show opposite rotation directions in the orientated plane perpendicular to the static geomagnetic field. This averaging will not occur if we consider only a half-plane water layer (still sited in the same homogeneous electrically conductive ground): the East and West half-planes will show different responses as can be seen on Fig. 7 for measurements simulated in a 1 Ω m medium at the magnetic equator (with a 50,000 nT magnitude). The observed differences are in the order of 20–25% of the maximum response value. Hence for 2D or 3D modelling and inversion, it will be important to use the proper exact formula when quite conductive environments are considered.

9. A field example over a highly conductive medium

As part of a comprehensive study of geophysical methods applied to groundwater exploration

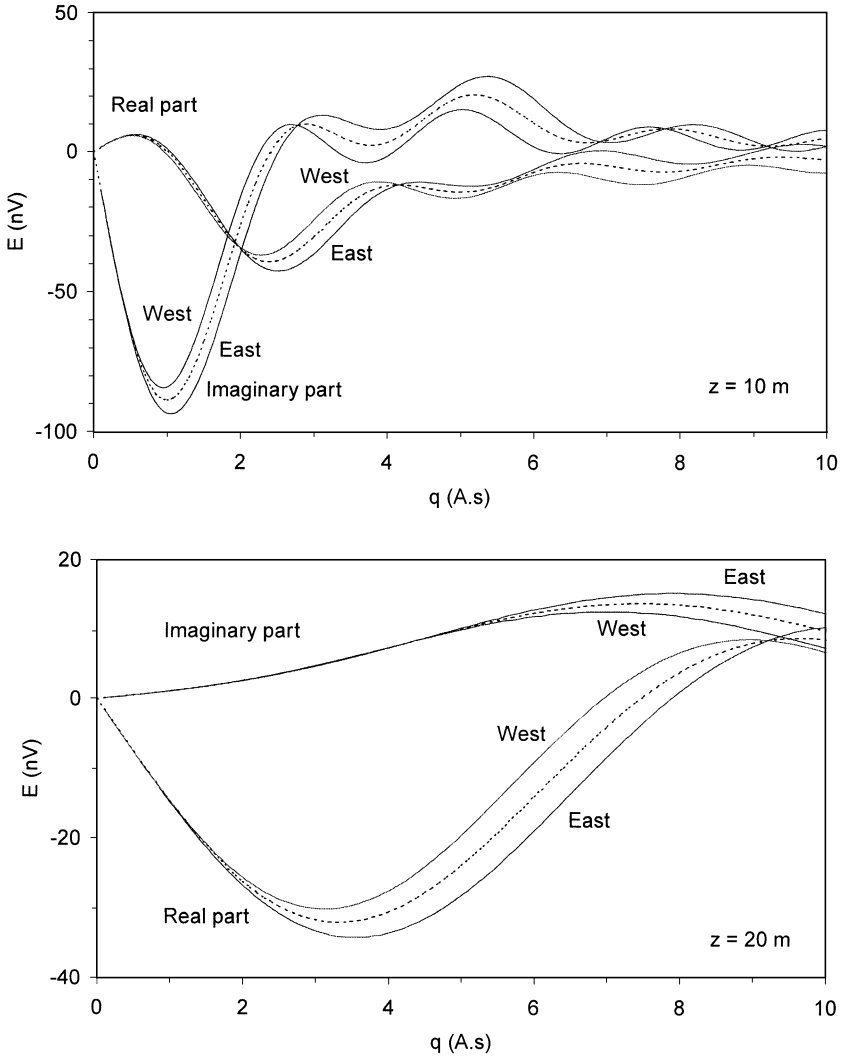

Fig. 7. Comparison of the responses of East and West half-plane thin (1 m) water layers at 10 (top) and 20 m (bottom) depth within a 1 Ω m half-space at 0° inclination; dashed line is the average, equal to half of a full plane thin water layer.

and resource assessment (EEC-INCO Project No. 18CT960122) a number of SNMR soundings have been performed in Cyprus during spring 1999. The site of the example presented hereafter is located in the Xylophagou area along the south–east coast, a few hundred meters from the Mediterranean sea; a square loop with 75 m long sides was used as an antenna; the geomagnetic field inclination was 40° and its amplitude was 45,300 nT corresponding to a Larmor frequency of 1927 Hz. From a time-domain electromagnetic sounding the electrical resistivity has been found to be about 2 Ω m for at least the first hundred meters. Such a low resistivity value is corroborated by the phase variation of the SNMR sounding: as the

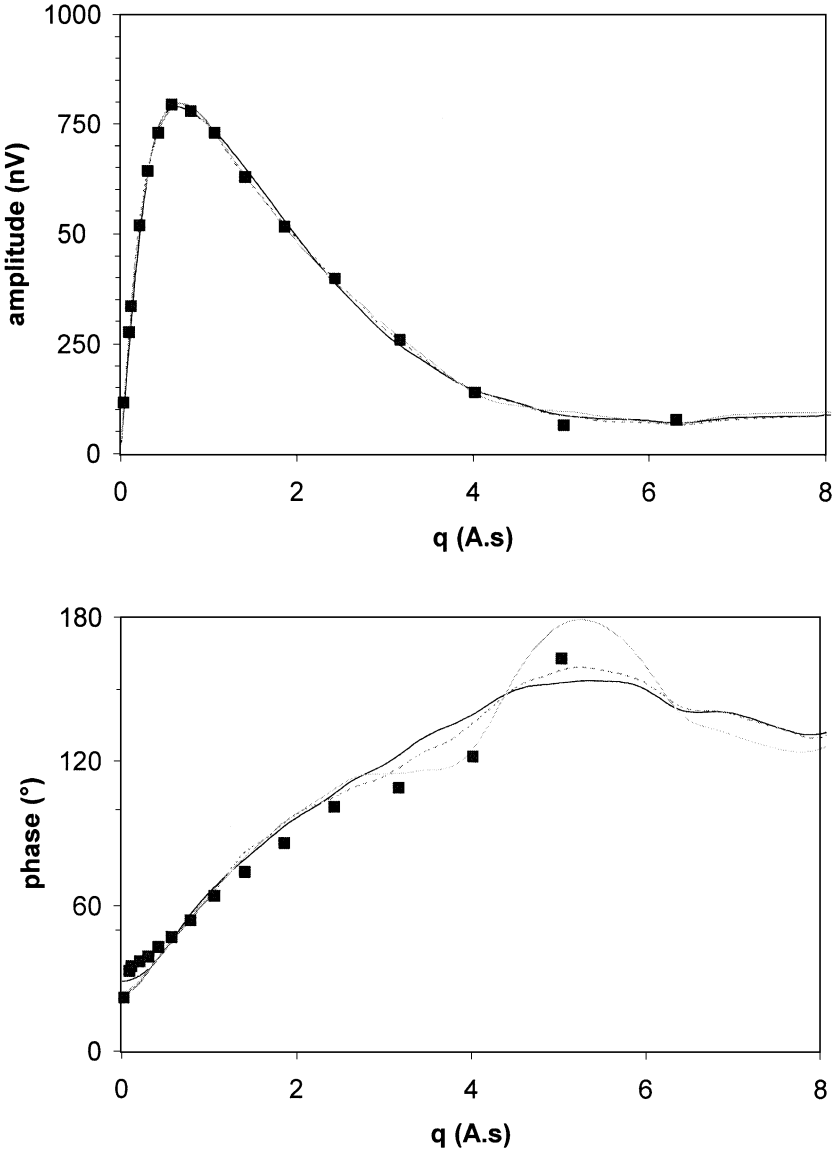

Fig. 8. Amplitude (top) and phase (bottom) of field data (dots) and modelled data (lines) for a proton magnetic resonance sounding example near the coast of the Cyprus island; the three lines correspond to the three water content distibutions plotted in Fig. 9.

excitation pulse moment increases, the phase increases by about 100°. Hence the 1D interpretation has been performed with a homogeneous 2 Ω m half-space hypothesis; for the modelling, a circular loop with 42.3 m radius has been used, providing an area identical to that of the square loop used in the field.

The field data and the modelled response are compared in Fig. 8. The inferred water content distributions are plotted in Fig. 9. The oscillations seen on the modelled curves, especially the phase ones, are not due to computation noise but to constructive and destructive interference between the responses from various depths.

The fact that the first few phase values at the lowest excitation pulse moments (except for the very first one that is probably less well defined because a lower signal amplitude) point towards a non-zero limiting value is indicative of the absence of water near the surface. The grey curves in Fig. 8 correspond to two possible water content distributions with varying values for multiple layers that are taken to be 1 m thick down to 20 m and 2.5 m thick thereafter; the dashed line corresponds to a best fit inversion made with only the amplitude data while the solid line corresponds to a best fit inversion made with both the amplitude and phase data; from these inversion results the groundwater is seen as being confined between 3 and 23 m. The black curve corresponds to a constant water content, namely 40%, within the same depth interval. No good fit can be obtained if a non-negligible water content is supposed below 23 m depth. The water-bearing layer is a limestone bed; its depth extent has been found to be larger in other locations, but there is no evidence at this site to support or contradict a lithology change at such a depth.

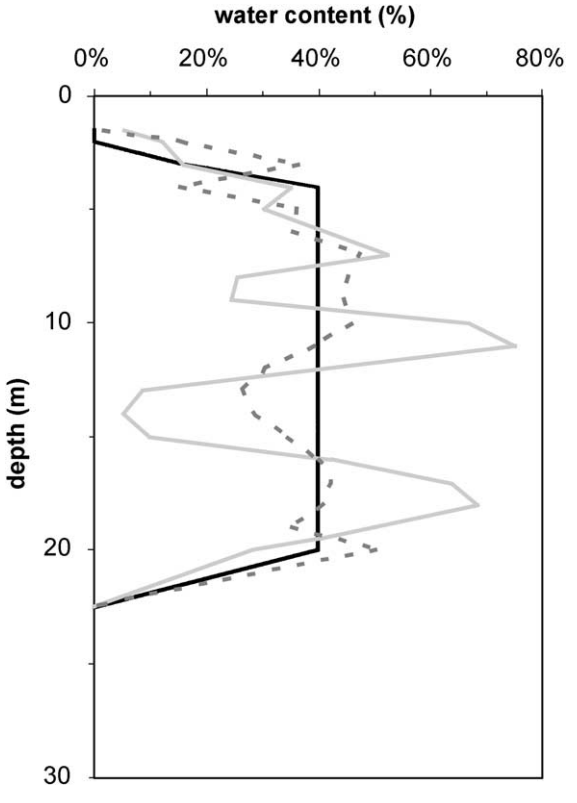

Fig. 9. Water content distribution inferred for the proton magnetic resonance sounding example; the black curve corresponds to a constant 40% content from 3 to 20 m depth while the grey curves correspond to 1 m thick layers with varying water content.

It should be noted that assuming 0.3 Ω m as the fluid resistivity (sea water), the 40% water content indeed leads to a resistivity value close to 2 Ω m when using Archie's law with a coefficient equal to 1 and an exponent equal to 2.

10. Conclusion

The exact equations for the modelling of magnetic resonance measurements made over a conductive medium have been presented in the theoretical framework used by geophysicists for frequency-domain electromagnetic methods. For horizontally layered conductivity and water content distributions little differences in the modelling results are observed compared to those obtained with the approximate formula used to date (Shushakov, 1996).

However for two-dimensional or three-dimensional models significant differences may occur as shown for a 2D water distribution within a homogenous electrically conductive ground. It will then be important to use the exact formulas.

Acknowledgements

The comments and suggestions made by Professor Peter Weidelt and Dr. Dave Fitterman have greatly helped in improving the clarity of the wording.

References

Anderson, W.L., 1979. Numerical integration of related Hankel transforms of orders 0 and 1 by adaptive digital filtering. Geophysics 44, 1287–1305.

Anderson, W.L., 1989. A hybrid fast Hankel transform algorithm for electromagnetic modelling. Geophysics 54, 263–266.

Chave, A.D., 1983. Numerical integration of related Hankel-transforms by quadrature and continued fraction expansion. Geophysics 48, 1671–1686.

Kaufman, A.A., Keller, G.V., 1983. Frequency and Transient Soundings. Elsevier.

Ryu, J., Morrison, F., Ward, S., 1970. Electromagnetic fields about a loop source of current. Geophysics 35, 862–896.

Shushakov, O.A., 1996. Groundwater NMR in conductive water. Geophysics 61, 998–1006.

Trushkin, D.V., Shushakov, O.A., Legchenko, A.V., 1995. Surface NMR applied to an electroconductive medium. Geophysical Prospecting 43, 623–633.

Wait, J.R., 1982. Geo-Electromagnetism. Academic Press.

Weichman, P.B., Lavely, E.M., Ritzwoller, M.H., 1999. Surface nuclear magnetic resonance imaging of large systems. Physical Review Letters 82, 4102–4105, May 17, 1999.